Developmental Biology 386 (2014) 111–122

Contents lists available at ScienceDirect

Developmental Biology

journal homepage: www.elsevier.com/locate/developmentalbiology

Zebrafish nephrogenesis is regulated by interactions between retinoic acid, *mecom*, and Notch signaling ☆

Yue Li, Christina N. Cheng, Valerie A. Verdun, Rebecca A. Wingert *

Department of Biological Sciences, University of Notre Dame, 100 Galvin Life Sciences, Notre Dame, IN 46556, USA

ARTICLE INFO

Article history:
Received 16 August 2013
Received in revised form
19 November 2013
Accepted 20 November 2013
Available online 3 December 2013

Keywords:
Pronephros
Nephrogenesis
Segmentation
Retinoic acid
mecom
Notch

ABSTRACT

The zebrafish pronephros provides a conserved model to study kidney development, in particular to delineate the poorly understood processes of how nephron segment pattern and cell type choice are established. Zebrafish nephrons are divided into distinct epithelial regions that include a series of proximal and distal tubule segments, which are comprised of intercalated transporting epithelial cells and multiciliated cells (MCC). Previous studies have shown that retinoic acid (RA) regionalizes the renal progenitor field into proximal and distal domains and that Notch signaling later represses MCC differentiation, but further understanding of these pathways has remained unknown. The transcription factor *mecom* (*mds1/evi1 complex*) is broadly expressed in renal progenitors, and then subsequently marks the distal tubule. Here, we show that *mecom* is necessary to form the distal tubule and to restrict both proximal tubule formation and MCC fate choice. We found that *mecom* and RA have opposing roles in patterning discrete proximal and distal segments. Further, we discovered that RA is required for MCC formation, and that one mechanism by which RA promotes MCC fate choice is to inhibit *mecom*. Next, we determined the epistatic relationship between *mecom* and Notch signaling, which limits MCC fate choice by lateral inhibition. Abrogation of Notch signaling with the γ-secretase inhibitor DAPT revealed that Notch and *mecom* did not have additive effects in blocking MCC formation, suggesting that they function in the same pathway. Ectopic expression of the Notch signaling effector, Notch intracellular domain (NICD), rescued the expansion of MCCs in *mecom* morphants, indicating that *mecom* acts upstream to induce Notch signaling. These findings suggest a model in which *mecom* and RA arbitrate proximodistal segment domains, while MCC fate is modulated by a complex interplay in which RA inhibition of *mecom*, and *mecom* promotion of Notch, titrates MCC number. Taken together, our studies have revealed several essential and novel mechanisms that control pronephros development in the zebrafish.

Introduction

Vertebrate kidney organogenesis proceeds through the formation and regression of several successive structures, each comprised of excretory units known as nephrons (Dressler, 2006). The first structure is the pronephros, composed of rudimentary nephrons formed next to the nephric cord, a bilateral epithelial tubule derived from the intermediate mesoderm (IM). Whereas the pronephros is a vestigial organ in mammals, it serves as the embryonic excretory organ in lower vertebrates such as fish and frogs (Dressler, 2006). During mammalian development, a mesonephros forms posteriorly to the pronephros and functions transiently in fetal life, then subsequently a third structure, the metanephros, is formed that functions as the definitive adult kidney (Dressler, 2006). The metanephros arises when the ureteric bud grows out of the caudal end of the nephric duct, invades the surrounding metanephric mesenchyme, and induces a mesenchyme-to-epithelial transition (MET) in cell aggregates adjacent to the ureteric bud tips (Little and McMahon, 2012). Mesenchymal cells undergoing MET form a polarized renal vesicle, which develops sequentially into a comma-shaped body, S-shaped body, and eventually into a segmented nephron tubule (Little and McMahon, 2012). Highly elaborate branching of the ureteric bud along the radial axis of the metanephric mesenchyme generates a complicated network within the collecting duct system, with thousands of nephrons situated in an intricate, arborized three-dimensional arrangement.

Abbreviations: CS, corpuscle of Stannius; DE, distal early; DEAB, 4-diethylaminobenzaldehyde; DL, distal late; dpf, days post-fertilization; G, glomerulus; hpf, hours post-fertilization; *mecom*, *mds1/evi1 complex*; IM, intermediate mesoderm; MCC, multiciliated cell; MET, mesenchymal to epithelial transition; N, neck; NICD, Notch intracellular domain; PCT, proximal convoluted tubule; PD, pronephric duct; PM, paraxial mesoderm; PST, proximal straight tubule; RA, retinoic acid; RARE, retinoic acid response element

* Corresponding author. Fax: +1 574 631 7413.
E-mail address: rwingert@nd.edu (R.A. Wingert).

0012-1606/$ - see front matter © 2013 The Authors. Published by Elsevier Inc. All rights reserved.
http://dx.doi.org/10.1016/j.ydbio.2013.11.021

There is currently a limited understanding of how nephron tubules are patterned into segments, due in part to the complexity of mammalian nephrogenesis and kidney anatomy (Costantini and Kopan, 2010). However, in recent years the zebrafish has emerged as a useful vertebrate model to study nephron segmentation (Gerlach and Wingert, 2013). Zebrafish embryos form a pronephros with two nephrons that originate from bilateral stripes of IM, from which renal progenitors are generated (Drummond, et al., 1998). The rostral renal progenitors give rise to a single glomerulus that the nephrons share, while the remaining renal progenitors undergo a MET to generate tubules that fuse at the cloaca (Drummond, et al., 1998; Serluca and Fishman, 2001). Gene expression profiling, largely based on genes encoding solute transporter proteins that account for the exquisite functions of each segment, revealed that the zebrafish pronephros segment composition is analogous to other vertebrates (Wingert, et al., 2007; Wingert and Davidson, 2008; Wingert and Davidson, 2011). By 24 hours post-fertilization (hpf), the zebrafish pronephros exhibits eight segments: the glomerulus (G), neck (N), proximal convoluted tubule (PCT), proximal straight tubule (PST), distal early (DE), corpuscle of Stannius (CS), distal late (DL), and pronephric duct (PD) (Fig. 1A) (Wingert, et al., 2007).

Studies of zebrafish nephrogenesis have identified several transcription factors and signaling pathways that are crucial for renal progenitor patterning (Gerlach and Wingert, 2013). Among them, the diffusible morphogen retinoic acid (RA) is essential for proximal–distal regionalization of the renal progenitor field (Wingert, et al., 2007; Wingert and Davidson, 2011). In target tissues, RA regulates gene expression by entering the nucleus and binding to its nuclear receptors, which upon RA interaction directly bind to retinoic acid response elements (RARE) to modulate transcription (Duester, 2008). Zebrafish genetic mutants lacking key RA synthesizing enzymes or wild types treated with diethylaminobenzaldehyde (DEAB), a chemical that blocks RA biosynthesis, develop a pronephros with reduced proximal segments and expanded distal segments (Wingert et al., 2007; Wingert and Davidson, 2011). These studies established that RA induces proximal segment identities during the early somite stages, and may directly repress distal segments. Downstream of RA, the terminal boundaries of each segment are defined by the expression of domain-specific genes and appear to be controlled by the activity of multiple downstream transcription factors, presently known to include *irx3b* and *hnf1β* (Wingert and Davidson, 2011; Naylor et al., 2013). Further, Notch signaling restricts MCC number by modulating the fate choice between transporting epithelium and MCC during mid-to-late somitogenesis (Ma and Jiang, 2007; Liu et al., 2006). Despite these findings, many questions remain concerning how each nephron segment is precisely established during nephrogenesis – including the identity of other key factors involved in segmentation.

In searching for additional factors that may control nephron segmentation, we identified the zinc finger transcription factor *Mecom* as an intriguing candidate gene. *Mecom* is a splice variant of the *ecotropic virus integration site 1* (*Evi1*) and *myelodysplastic syndrome 1* (*Mds1*) genes, which results in an N-terminal extension of the Evi1 protein (Wieser, 2007). Targeted disruptions that result in the loss of both transcripts cause embryonic lethality in mice associated with defects in neural, heart, and blood development – which suggests that this locus has multiple essential roles during ontogeny (Goyama, et al., 2008; Wieser, 2007; Hoyt, et al., 1997). More recent work has demonstrated that *Mecom* is required for long-term hematopoietic stem cell maintenance (Zhang, et al., 2011).

With respect to vertebrate kidney development, transcripts encoding *Mecom* have been detected in the pronephros distal tubule and duct in *Xenopus* (Mead, et al., 2005) and zebrafish *mecom* has also been reported in the pronephros (Wingert, et al., 2007; Wingert and Davidson, 2011). In the zebrafish, *mecom* is initially expressed in the renal progenitor field, but its domain changes dynamically during nephrogenesis (Wingert et al., 2007; Wingert and Davidson 2011). *mecom* marks a broad caudal domain in early stages, then is later restricted to the DL and PD at 24 hpf. A genome-scale *in situ* analysis of mammalian transcriptional regulatory factors reported expression of murine *Mecom* in nascent nephron S-shaped bodies in the developing metanephric kidney (Yu et al., 2012), thus further suggesting it could be involved in nephron patterning across vertebrates. However, the mechanism of how *mecom* modulates vertebrate nephron segmentation and the signaling pathways that may interact with *mecom* in renal progenitors remain unclear.

Through the present study, we found that interactions between RA, *mecom*, and Notch signaling are essential for zebrafish pronephros development. We show that *mecom* expression is extremely dynamic in zebrafish renal progenitors and is negatively regulated by RA. Using both loss and gain-of-function approaches, we found that *mecom* is necessary for proper DL segment formation, and that the absence of *mecom* activity expands the PST segment and MCC numbers. Moreover, *mecom* and RA have opposing roles in PST and DL formation, as *mecom* morphants treated with exogenous RA had a more expanded PST and an abrogated DL, while DEAB treatment rescued segmentation in *mecom* morphants. Consequently, we discovered a previously unappreciated role for RA in MCC development, since DEAB treatment prevented MCC formation while *mecom* knockdown in DEAB-treated embryos rescued MCCs. These data indicate that RA regulates MCC fate choice by inhibiting *mecom*. Furthermore, we established the epistatic relationship between Notch signaling and *mecom* during MCC differentiation, where *mecom* acts upstream to promote Notch activity. Taken together, our data suggest a model in which *mecom* and RA function during early nephrogenesis stages to arbitrate proximodistal segment pattern, and reveal that MCC fate choice is modulated by a complex interplay between RA, *mecom*, and Notch signaling to precisely define the MCC domain and density in the nephron.

Materials and methods

Zebrafish husbandry and ethics statement

Zebrafish were maintained in the Center for Zebrafish Research at the University of Notre Dame Freimann Life Science Center. Wild type embryos were raised and staged as described (Kimmel et al., 1995). The Institutional Animal Care and Use Committee at the University of Notre Dame supervised experimental procedures under protocols 13-021 and 16-025.

Morpholino knockdown, cRNA synthesis, and heat shock experiments

All morpholinos were purchased from Gene Tools, LLC (Philomath, OR), and were solubulized as recommended and stored at a 4 mM concentration. The *mecom* morpholino *e1SD* (5′-CTGAGTGACTTACATATGAAGGGCT-3′) was designed to target the splicing donor site of zebrafish *mecom* (XM_001920912) exon 3, and *e1SA* (5′-TTGTGGCAGACCTCACGACGGTGTT-3′) targets the splicing acceptor of exon 4. The *mecom* mismatch morpholinos (5′-CTGATTGACGTACAAATGATGGGCA-3′ and 5′-TTGTAGCAGGCCTCGCGACTGTGTA-3′) were used as controls. A combination of *mecom e1SD* and *e1SA* morpholinos produced fully penetrant effects and was used for all *mecom* knockdown experiments. One-cell stage wild type embryos were injected with 1–5 nl 0.2 mM *mecom* morpholinos and raised to the desired stages at 28 °C. For gene expression analysis, embryos were fixed in 4% paraformaldehyde/1 × PBST and stored in methanol at −20 °C. Synthetic *mecom* cRNA was synthesized from a *mecom.*

pCS2 plasmid using the mMessage mMachine sp6 kit (Ambion). For rescue experiments, one-cell stage embryos were co-injected with 1–5 nl of 5 ng/μl *mecom* cRNA and 0.2 mM *mecom* morpholinos. For NICD heat shock experiments, embryos were incubated at 37 °C for 1 h beginning at 90% epiboly, allowed to develop to the desired stage, fixed and processed for WISH, and then ultimately genotyped as described (Scheer and Campos-Ortega, 1999).

RT-PCR

RNA was extracted from *mecom* morphant and wild type embryos at 24 hpf with Trizol reagent (Invitrogen) according to the manufacturer's instructions. RT-PCR was performed using the SuperScript First-Strand Synthesis System (Invitrogen). To confirm mis-splicing of *mecom* in morphant embryos, PCR primers were

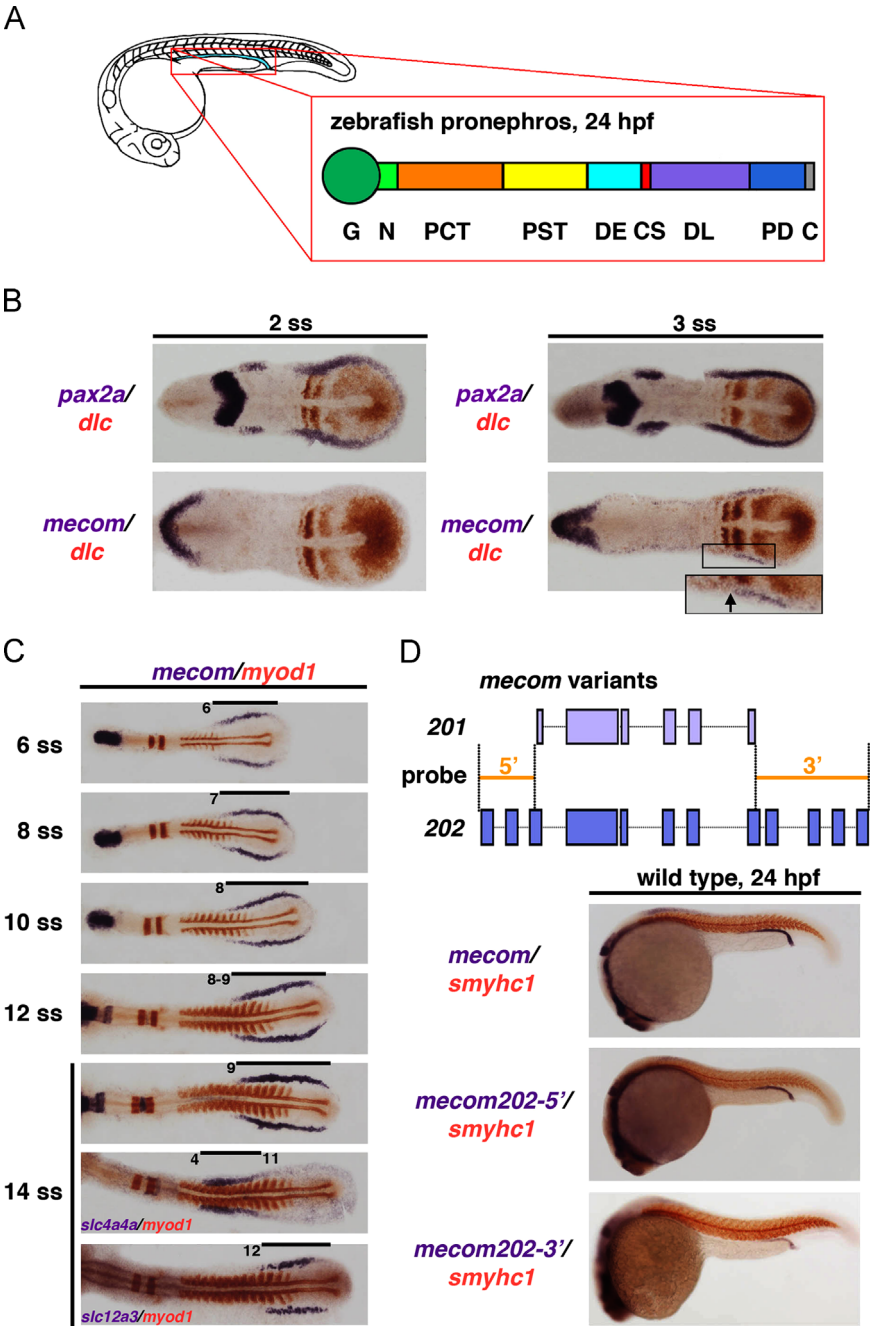

Fig. 1. *mecom* transcripts mark an early caudal domain of the renal progenitors, and the *mecom* expression domain is dynamic during nephrogenesis. (A) Schematic depictions of zebrafish pronephros at 24 hpf, shown in lateral view. Enlargement represents segmental organization of the nephron at 24 hpf. Abbreviations: G (glomerulus), N (neck), PCT (proximal convoluted tubule), PST (proximal straight tubule), DE (distal early), CS (corpuscle of Stannius), DL (distal late), PD (pronephric duct), and C (cloaca). (B) At the 2 and 3 somite stages, the renal progenitor field was labeled by *pax2a* (purple) and forming somites were marked by *dlc* (red). Onset of *mecom* expression in renal progenitors could be detected at the 3 somite stage, in a caudal domain exclusive to the *dlc*-expressing rostral domain. Inset shows non-overlapping expression territory of *dlc* (red) and *mecom* (purple) at 3 somites in the renal progenitor field. (C) Expression of *mecom* (purple) and *myod1* (red) at various time points between 6 and 14 somite stages in wild types. At 14 somites, the expression domains of solute transporters *slc4a4a* and *slc12a3* indicate premature patterning of the pronephros proximal versus distal segment regions. (D) Upper panel: genomic structure of zebrafish *mecom202* (dark purple, bottom) and *mecom201* (*evi1*) (light purple, top). The *mecom202-5′* and *mecom202-3′* riboprobes (orange filled lines) were designed to distinguish *mecom202* and *mecom201* transcripts by targeting the 5′ and 3′ region exclusively present in *mecom202* transcripts. Lower panels: in 24 hpf wild type embryos, WISH using a full-length *mecom202* probe and *mecom202*-specific probes showed that *mecom* expression was restricted to the DL and PD regions of the pronephros.

designed to specifically amplify the *mecom* mRNA region corresponding to 180 bp of sequence spanning exons 3 and 4 (exon 3 forward primer 5′-AACTTGCAGAGGCATATCCG-3′, and exon 4 reverse primer 5′-GGCAGAGATTGGAGAACTGC-3′). Primers located in introns 3–4 were used to amplify a 190 bp intronic fragment (introns 3–4 forward primer 5′-CCTATGCTAGGGACACCTGG-3′, and introns 3–4 reverse primer 5′-GCCTCGAAAACGTAGAATGC-3′). To assess the exon 3-introns 3–4 fusion in *mecom* morphants, the exon 3 forward primer and introns 3–4 reverse primer were used in combination to amplify a ~1.3 kb cDNA fragment.

Dextran injection

To assay kidney function, 40 kDa fluorescent dextran-FITC (Invitrogen) was injected into an axial somite of 1-phenyl-2-thiourea (PTU) treated wild type embryos or *mecom* morphants that were anesthetized with 0.02% tricaine at 48 hpf. Embryos were revived and incubated in PTU in the dark until later time points for observation. Dextran clearance was observed with a fluorescent microscope at 72 hpf and 98 hpf.

Benzidene staining

o-Dianisidine stock was made by dissolving 0.07 g of o-dianisidine (Sigma D9134) in 50 ml of 100% ethanol. Live embryos were incubated in the dark for 15 min in a working solution comprised of 2 ml o-dianisidine stock, 500 µl of 0.1 M sodium acetate pH 4.5, 2 ml of distilled water, and 100 µl of hydrogen peroxide. Embryos were rinsed three times in E3 and then fixed in 4% PFA for scoring and imaging.

Chemical treatments

RA and DEAB (Sigma-Aldrich) were dissolved in 100% DMSO to make 1 M stocks and the aliquots were stored at −80 °C (Wingert, et al., 2007). For RA treatments, tailbud stage embryos were incubated in 1×10^{-7} M RA/DMSO made with E3 embryo media in the dark until 24 hpf, washed three times with E3, then fixed. For DEAB treatments, the embryos were incubated in 1.6×10^{-5} M DEAB/DMSO diluted in E3 media from 75% epiboly to 24 hpf. Control embryos were allowed to develop in 1×10^{-7} M or 1.6×10^{-5} M DMSO over corresponding developmental intervals. DAPT was dissolved in DMSO to make a 10 mM stock and stored at −80 °C. Bud stage embryos were incubated in 100 µM DAPT/DMSO or DMSO alone in E3 media to 24 hpf at 28 °C in the dark. These chemical treatments were fully penetrant and produced consistent results.

WISH

For our reported WISH expression studies and images, representative results are provided based on analysis of at least 20 embryos, and gene expression domains as reported by somite boundaries were based on counts of at least five separate embryos for accuracy. Zebrafish WISH was performed as previously described (Wingert et al., 2007). To generate antisense probes for *pax2a*, *dlc*, *egr2a*, *mecom*, *myod1*, *smyhc1*, *slc4a4a*, *slc20a1a*, *trpm7*, *clcnk*, *slc12a1*, *slc12a3*, *wt1b*, and *nr5a1a*, we used IMAGE clone template plasmids for *in vitro* transcription, as previously reported (Wingert et al., 2007; Wingert and Davidson, 2011). Probes for *odf3b* were transcribed from PCR templates amplified with primers (5′-ATGTCACCTGTGGATGTATG-3′ and 5′-AATTAACCCTCACTAAAGGGTTAATCTTCACC-3′). To distinguish *mecom* from other transcript variants, we generated antisense probes *mecom829* and *mecom555* targeting the first 829 bp and the last 555 bp fragments specifically present in *mecom* using PCR templates obtained with *mecom829* primers (forward: 5′-TGGATTTTGAGGGACAGGAG-3′ and reverse: 5′-AATTAACCCTCACTAAAGGGCATTGGGGCATTATGGGTAG-3′) and *mecom555* primers (forward: 5′-CTTTGAGTCTGGTTCGGAGC-3′ and reverse: 5′-AATTAACCCTCACTAAAGGGTTGGATTTCCAGTTGAAGGC-3′) respectively.

Cell counting and statistics

Quantification of MCC density in the pronephros was conducted by counting the number of MCCs in a length ranging from 50 µm to 150 µm per nephron. MCC density was determined by calculating the number of MCCs per 10 µm. At least 20 embryos were examined for each experiment. Student's *t*-test was applied for quantitative results.

Results

mecom delineates a dynamic caudal subdomain in the renal progenitor field

Based on the gene expression patterns of specific solute transporters, the molecular anatomy of the zebrafish pronephros consists of proximal and distal segments that are analogous to mammalian nephrons (Wingert, et al., 2007). Eight similar regions have been identified, including two proximal tubule domains (PCT, PST) and two distal tubule domains (DE, DL) (Fig. 1A). Prior studies have documented the appearance of *mecom* transcripts as occurring between the 6 and 8 somite stages during pronephros development (Wingert, et al., 2007; Wingert and Davidson, 2011). To further examine the onset of *mecom* expression in the renal progenitor field, we assessed the domain of *mecom* transcripts by performing double whole-mount *in situ* hybridization (WISH) with several combinations of riboprobes consisting of both segmentation and somitogenesis gene probes that would enable labeling of renal progenitor domains compared to the somite boundaries. To confirm the embryonic stage and define somite boundaries, emerging somites were labeled in embryos between 1 and 6 somites using *deltaC* (*dlc*), while embryos between 6 and 18 somites were labeled with *myogenic differentiation 1* (*myod1*).

The domain of renal progenitors was visualized based on the expression of *pax2a* (Fig. 1B) (Pfeffer et al., 1998). At the 2 somite stage, *mecom* expression was absent in the renal progenitor field, whereas transcripts were present in the developing brain (Figs. 1B and S1A). The onset of *mecom* expression in the renal progenitor domain occurred at the 3 somite stage, adjacent to where somite 4 was forming (Figs. 1B and S1A). In addition to marking the somites, the Notch ligand *dlc* is known to mark the rostral territory of the renal progenitors, which will eventually develop into the proximal segments in the pronephros (Wingert et al., 2007; Wingert and Davidson, 2011). During the onset of *mecom* expression, there was a clear delineation between the *dlc*-expressing rostral domain and the *mecom*-expressing caudal domain at the 3 somite stage (Fig. 1B, inset). Notably, the detection of non-overlapping domains of *dlc* and *mecom* at the 3 somite stage is the earliest proximodistal distinction that has been observed within the renal progenitor field during zebrafish pronephros development.

Between the 6 and 15 somite stages, dynamic *mecom* expression was observed in the developing pronephros. The domain of *mecom* transcripts gradually shifted toward the caudal end of the renal progenitor field (Figs. 1C and S1B). By 14 somites, premature pronephric segments were established: the proximal domain was labeled by the solute transporter *solute carrier family 4, member 4a* (*slc4a4a*), while the distal domain was marked by *solute carrier family 12* (*sodium/chloride transporters*), *member 3* (*slc12a3*) (Fig. 1C, lower

two panels). At this time point, *mecom* transcripts were detected throughout the distal domain and partially overlapped with the proximal domain (Fig. 1C). The progressive shifting of the *mecom* expression domain continued from 18 to 28 somite stages, until its expression became restricted to the DL and PD (Figs. 1D and S2). The presence of *mecom* transcripts in early renal progenitors, and its ongoing dynamic expression domain, suggested to us that *mecom* could be functioning at multiple times in developing renal progenitors.

In zebrafish, two *mecom* splice variants have been identified. The 3129 basepair (bp) *mecom202* (*mecom*, also known as *prdm3*) (Sun et al., 2008) possesses additional extensions in both the 5′ and 3′ ends of the 1807 bp *mecom201* (*evi1*). To distinguish the expression of *mecom202* from *mecom201*, we utilized the 5′ and 3′ end fragments present exclusively in *mecom202* transcripts and designed riboprobes *mecom202-5′* and *mecom202-3′* (Fig. 1D). WISH using a full-length *mecom* riboprobe indicated *mecom* was restricted in the DL and PD regions of the pronephros at 24 hpf, while *mecom202-5′* and *mecom202-3′* probes further demonstrated that the *mecom202* transcripts were expressed in the pronephros and restricted to the DL and PD at 24 hpf as well (Figs. 1D, S1, and S2).

mecom morphants exhibited renal edema and dysfunction

To assess the role of *mecom* in zebrafish pronephros segmentation, we performed morpholino knockdown studies. One-cell stage wild type embryos were injected with a *mecom* morpholino targeting the splice donor site of exon 3, the splice acceptor of exon 4, or a combination of these two morpholinos (Figs. 2A, S3A, and S3B). We found that the morpholino combination induced stronger phenotypes than either morpholino alone (Figs. 2A, S3A, and S3B). Based on these results, we co-injected the *mecom* splice morpholinos for the remainder of our studies on *mecom* loss of function. Next, we performed a series of RT-PCR experiments to assess changes in *mecom* mRNA splicing in co-injected morphant embryos compared to uninjected wild type controls. Primers were designed to amplify the *mecom* sequence spanning exon 3 and exon 4 to identify the properly spliced *mecom* mRNA fragment (Fig. 2A). We found that cDNA isolated from wild-type embryos contained *mecom* transcripts with the predicted exons 3–4 band size of 180 base pairs (bp), which indicated appropriate splicing between these exons (Fig. 2A). However, *mecom* morphant embryos injected with the combination of splice morpholinos showed low, if any, correctly processed *mecom* mRNA across exons 3–4 (Fig. 2A). This suggested that there was a significant reduction in normal *mecom* mRNA as a consequence of the morpholino injection. In *mecom* morphants, these primers failed to amplify a *mecom* cDNA product containing the entire introns 3–4 (data not shown), but this could be due to the size of that intron, which is predicted to be 4.4 kilobases (kb) in length.

To further address how the *mecom* transcript was processed in the morphants, we designed primers that would amplify smaller portions of the intronic interval. In *mecom* morphants, but not in wild type uninjected embryos, we detected the presence of transcripts corresponding to *mecom* introns 3–4 sequences (example in Fig. S3C, data not shown). Further, in *mecom* morphants we were able to amplify a 1.3 kb *mecom* cDNA sequence spanning the 3′ end of exon 3 and the 5′ end of introns 3–4; importantly, this intronic fragment contains a series of in-frame stop codons (data not shown). Thus, we hypothesize that the *mecom* morpholinos generate a mis-spliced mRNA that in turn results in a truncated Mecom protein. While we were unable to determine if *mecom* morphants retain the entire introns 3–4 after *mecom* transcript processing, our data nevertheless confirm that these splice junction *mecom* morpholinos lead to mis-spliced *mecom* mRNA.

Next, to broadly evaluate the role of *mecom* during zebrafish development, we followed the development of *mecom* morphants compared to control embryos injected with the mismatch morpholinos. At 30 hpf, *mecom* morphants showed pericardial edema, mild tail-axis curvature, and brain and eye defects (Fig. 2B). In contrast, wild type embryos injected with the mismatch morpholinos had no gross developmental abnormalities (Fig. 2B). At 50 hpf, *mecom* morphants displayed severe pericardial edema, suggesting possible pronephros dysfunction and fluid imbalance compared to wild types (Fig. 2B). Fluid accumulation could also result from cardiac defects and impaired circulation. However, the heart rate was normal in morphants compared with wild type embryos, circulation ensued normally at 24 hpf, and circulation continued to appear normal through 48 hpf (data not shown). To further scrutinize the circulation, we used benzidene staining, which labels hemoglobin in differentiated erythrocytes starting just after 32 hpf, and can more precisely assay if blood pooling transpired in *mecom* morphants (Fig. S4) (Wingert et al., 2004). We found that 8.6% (4/46) of *mecom* morphants had cranial blood pooling at 36 hpf, and that the incidence of this phenotype increased to 54.5% (12/22) of *mecom* morphants by 48 hpf, while no wild type embryos displayed a pooling phenotype (out of 51 animals assayed at these time points) (Fig. S4). Taken together,

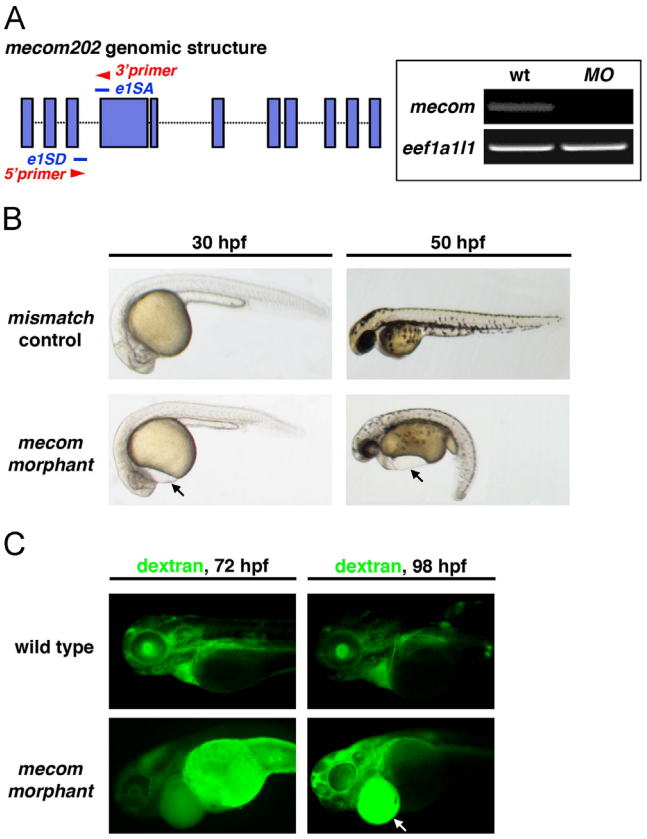

Fig. 2. *mecom* morphants exhibit pericardial edema and symptoms of renal failure. (A) Schematic indicates targeting sites of *mecom* morpholinos (blue lines) blocking splice sites of *mecom* mRNA between exons 3 and 4. Primers (red arrowheads) were designed to amplify the 180 bp linkage region between properly spliced exons 3 and 4. Right panels: cDNA isolated from wild type embryos showed the 180 bp band indicating proper splicing to remove intron 3. In contrast, amplification of this product was abrogated in *mecom* morphants. *eef1a1l1* was used as internal control. (B) *mecom* morphants showed gross developmental defects when compared with mismatch controls. Pericardial edema could be visualized at 30 hpf in *mecom* morphants indicating fluid accumulation (left panels). At 50 hpf, *mecom* morphants displayed severe pericardial edema and body curvature (right panels). (C) Fluorescent 40 kDa dextran was injected into a somite of wild types or *mecom* morphants at 48 hpf. A failure of renal clearance, indicated by dextran accumulation, was observed in the yolk and edema of *mecom* morphants at 72 and 98 hpf.

these data suggest the *mecom* knockdown is associated with circulation and/or vascular integrity defects that worsen over developmental time. We hypothesize that this contributed to the pericardial effusion phenotype in *mecom* morphants. To assess renal function in *mecom* knockdowns, we explored renal absorption and clearance properties with dextran tracing experiments. We injected 40 kDa dextran-FITC into the somites of wild type embryos or *mecom* morphants at 48 hpf. From 72 hpf to 98 hpf, wild types exhibited clearance of the fluorescent molecule, whereas abundant dextran-FITC accumulation was visualized in *mecom* morphants (Fig. 2C). These results indicate that *mecom* is necessary for proper development and function of the pronephros.

mecom knockdown induced PST specific expansion in the zebrafish pronephros

To further characterize nephron development in *mecom* morphants, we used double WISH with domain-specific markers and the somite marker *smyhc1* to precisely define each segment boundary relative to each somite. Interestingly, at 24 hpf, *mecom* morphants had expanded proximal tubules (Fig. 3). The pan-proximal marker *slc4a4a*, encoding an electrogenic Na^+ bicarbonate co-transporter, was expressed in the PCT and PST segments from somite 4 to 11 in wild-type embryos, whereas in *mecom* morphants, the *slc4a4a* domain was expanded from somite 4 to 14, and was rescued by *mecom* overexpression (62.5%, 20/32) (Figs. 3 and S5). Scrutiny of each segment domain revealed that expansion of the proximal tubule was attributed to an enlarged PST. The PCT expresses the sodium-dependent phosphate transporter *slc20a1a*, a domain that was situated adjacent to somites 4–8 in both wild type embryos and *mecom* morphants (Figs. 3 and S5). However, the PST labeled by the transient receptor potential cation channel gene *trpm7* was expanded from somites 9 to 14 in *mecom* morphants, while its expression in wild types was located next to somites 9 to 11 (Figs. 3 and S5). The PST expansion was consistent in more than 90% (49/52) of *mecom* morphants. In addition, more than 60% (23/36) of *mecom* morphants could be successfully rescued by co-injecting the *mecom* morpholinos along with full-length zebrafish *mecom* cRNA (Figs. 3 and S5). This result supports the conclusion that the segmentation defects observed after *mecom* knockdown are specific to the abrogation of mecom activity during nephrogenesis. The development of other proximal nephron cell types like the podocytes, or the interrenal lineage that emerges next to the podocytes, was not affected in *mecom* morphants (Fig. S6).

mecom morphants display PST expansion at the expense of the DL segment

To determine how the abnormal PST in *mecom* morphants affected distal segment patterning, we used double WISH with distal markers and *smyhc1*. Indeed, the increased PST in the morphant pronephros was accompanied by a robust reduction in the distal pronephros domain (Figs. 4 and S5). In wild type embryos at 24 hpf, the expression pattern of the chloride conductance channel gene *clcnk* could be seen in the DE, DL, and PD regions from somites 12 to 18 (Figs. 4 and S5). In contrast, the *clcnk* expression domain was reduced in the *mecom* morphants, being located from somites 15 to 18 starting adjacent to somite 15; however, this aberrant phenotype was rescued by *mecom* transcript overexpression (66.7%, 22/33) (Figs. 4 and S5). The DE domain marked by *slc12a1*, which encodes a $Na^+/K^+/Cl^-$ co-transporter, had a similar length in wild types and *mecom* morphants (Figs. 4 and S5). Surprisingly, the distal pronephros region was reduced specifically at the cost of the DL segment. The DL domain indicated by *slc12a3*, a Na^+/Cl^- transporter gene, showed a significant reduction in *mecom* morphants and was restricted to somites 17–18, whereas wild type embryos showed *slc12a3* expression from somites 14 to 17 (Figs. 4 and S5). The abrogation of the DL domain was not associated with heightened cell death in this domain at 24 hpf based on acridine orange staining (data not shown). Finally, we found that the DL segment formation was rescued in nearly 70% (26/37) of embryos that were co-injected with *mecom* morpholinos and *mecom* cRNA (Figs. 4A and S5), further supporting the specificity of *mecom* morpholinos. We conclude from these findings that *mecom* is essential for normal nephron segmentation, such that *mecom* activity promotes the DL and restricts the PST.

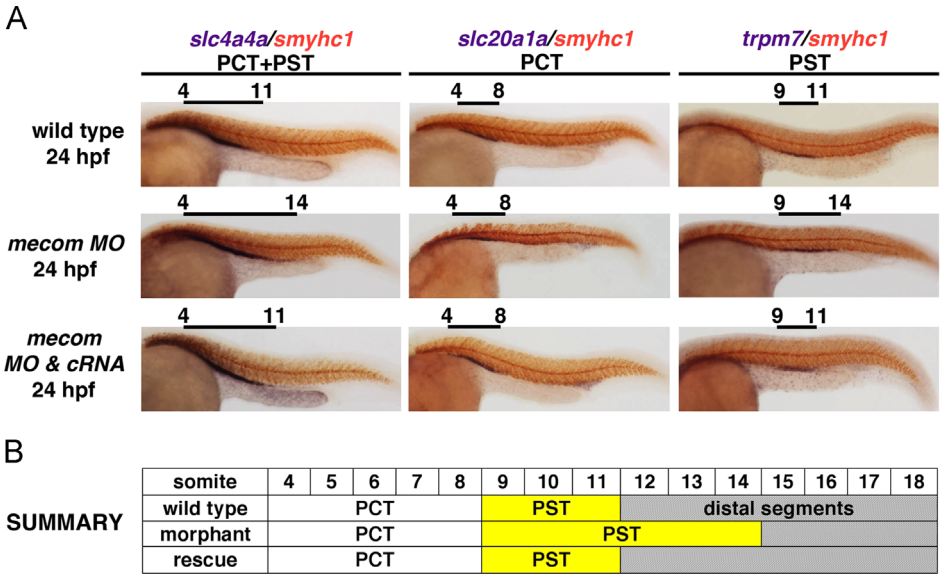

Fig. 3. *mecom* knockdown leads to an expanded PST segment. (A) At 24 hpf, WISH indicates proximal segments marked by *slc4a4a* elaborated in *mecom* morphants. Within proximal domains, PCT labeled by *slc20a1a* was not affected compared with wild type embryos. Knockdown of *mecom* induced a 3-somite expansion in *trpm7*-expressing PST in morphant pronephros at 24 hpf, which could be rescued by co-injecting *mecom* cRNA along with *mecom* morpholinos. (B) Schematic summary of proximal segment organization in wild type, *mecom* morphant, and *mecom* rescued embryos, with PST alterations highlighted in yellow. Abbreviations: PCT (proximal convoluted tubule), and PST (proximal straight tubule).

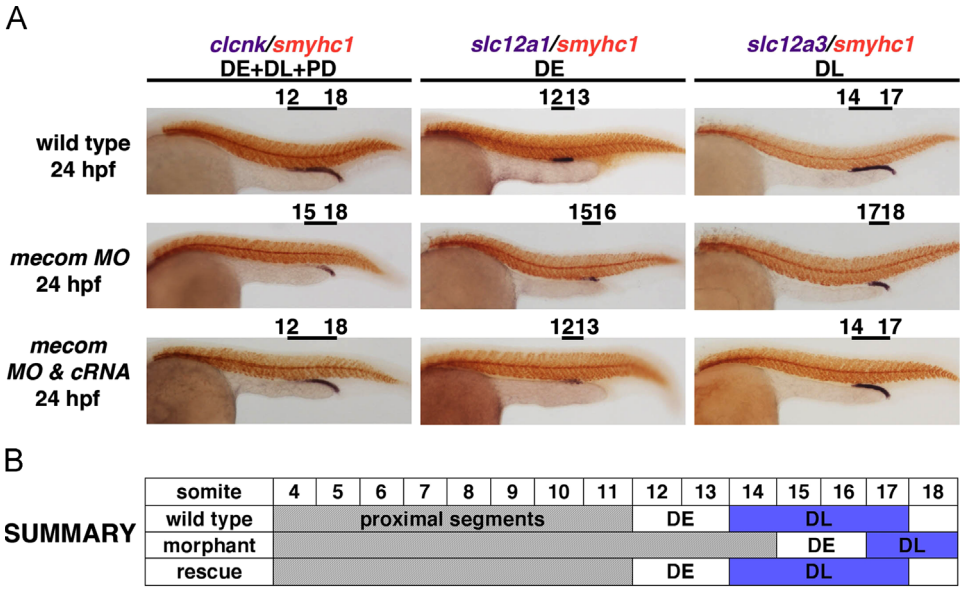

Fig. 4. *mecom* knockdown leads to the formation of a reduced DL segment. (A) WISH using distal segment markers showed a 3-somite reduction in DL region by 24 hpf. The distal segments and pronephros ducts were labeled by *clcnk*. Expression of *slc12a1* and *slc12a3* marked the DE and DL respectively. Pronephros segment boundaries were evaluated relative to the somites, which were shown by *smyhc1* expression (red). The reduced DL could be ameliorated by co-injection of *mecom* morpholino and *mecom* cRNA. (B) Schematic depiction of distal segment alterations, with DL domains highlighted in orchid. Abbreviations: DE (distal early), DL (distal late), and PD (pronephric duct).

RA negatively regulates mecom during pronephros segmentation

Next, we sought to identify possible developmental pathways relative to *mecom* in establishing the pronephric segmentation pattern. RA signaling plays important roles during segmentation: RA is required to induce proximal segments and to prevent distal segment expansion at early somitogenesis stages (Wingert et al., 2007; Wingert and Davidson, 2011). To further explore the relationship between *mecom* and RA signaling, we treated wild type embryos and *mecom* morphants with exogenous all-trans RA at the concentration of 1×10^{-7} M from bud stage to 24 hpf, and examined segmentation changes using WISH (Figs. 5 and S7). At this RA dosage and time window, wild type embryos developed a minor 'proximalized' pronephros phenotype with an expanded PST, indicated by *trpm7* expression, and a reduced DL segment marked by *slc12a3* (Figs. 5 and S7). However, at the same treatment condition, *mecom* morphants displayed a severe 'proximalized' pronephros indicated by the expansion of the *trpm7* expressing PST domain throughout the entire tubule and an almost complete loss of the *slc12a3* expressing DL segment (Figs. 5 and S7). Furthermore, as shown previously (Wingert et al., 2007), treating wild types with DEAB, an inhibitor of RA *aldehyde dehydrogenase* (*aldh*) synthesizing enzymes, resulted in a 'distalized' pronephros with an expanded DL and reduced PST (Figs. 5 and S7). When compared to *mecom* morphants or *mecom* morphants treated with RA, *mecom* morphants incubated with DEAB showed a partially reduced PST, as shown by *trpm7* expression from somites 9 to 13, and partially expanded *slc12a3* expression from somites 15 to 17 (Figs. 5 and S7). Altogether, these results show that *mecom* and RA have antagonistic activities in PST and DL formation: *mecom* inhibits the PST while RA promotes the PST, and *mecom* promotes the DL while RA inhibits the DL.

Based on these findings, we hypothesized that RA could negatively regulate *mecom*, which would provide a mechanism to account for the patterning change in the PST and DL segments. Interestingly, RA treatment beginning at 60% epiboly has been shown to reduce the *mecom* expression domain at the 6–8 somite stage, while DEAB exposure beginning at this time leads to an expansion of the *mecom* domain at the 6–8 somite stage – changes that correlate with reduced and expanded distal segments, respectively (Wingert et al., 2007). To further assess the relationship between RA signaling and *mecom*, wild type embryos were treated with RA or DEAB and *mecom* expression was evaluated using WISH (Figs. 6A and S7). Wild type embryos treated with RA showed a dramatically reduced *mecom* expression domain at 24 hpf, while embryos treated with DEAB had a dramatically expanded *mecom* domain, consistent with the notion that RA negatively regulates *mecom* expression during nephrogenesis (Figs. 6A and S7).

The activities of RA and mecom also regulate epithelial cell fate choice in tubule segments

In the zebrafish pronephros, intercalated along the PCT, PST, DE, and the anterior-most DL transporting epithelia are distinct multiciliated cells (MCCs), which can be evaluated based on the expression of various ciliogenesis genes, such as *odf3b*, via WISH (Ma and Jiang, 2007; Liu et al., 2006). How the MCC domain is defined within the renal progenitor field has yet to be understood, but MCC cell fate choice is limited through Notch signaling (Ma and Jiang, 2007; Liu et al., 2006). Interestingly, we found that *mecom* morphants exhibited an expanded MCC domain and a noticeable overall increase of MCC density at 24 hpf (Figs. 6B, S7, and S8). These observations indicate that *mecom* negatively regulates MCC development.

While RA is vital for patterning pronephros segmentation (Wingert et al., 2007; Wingert and Davidson, 2011), prior studies have not addressed how RA might affect MCC formation. Given the relationship between RA and *mecom*, we assessed whether RA is also involved in MCC patterning. Wild type embryos were treated with 1×10^{-7} M all-trans RA from tailbud stage to 24 hpf. The RA-treated embryos had a caudal expansion of the MCC domain (Figs. 6B and S7). When *mecom* morphants were treated with the same dosage of RA during this time window, they showed a slightly further expanded MCC domain (Figs. 6B and S7). These data suggested that RA has dual roles in patterning of the MCC domain and stimulating MCC formation, possibly via the inhibition of *mecom*.

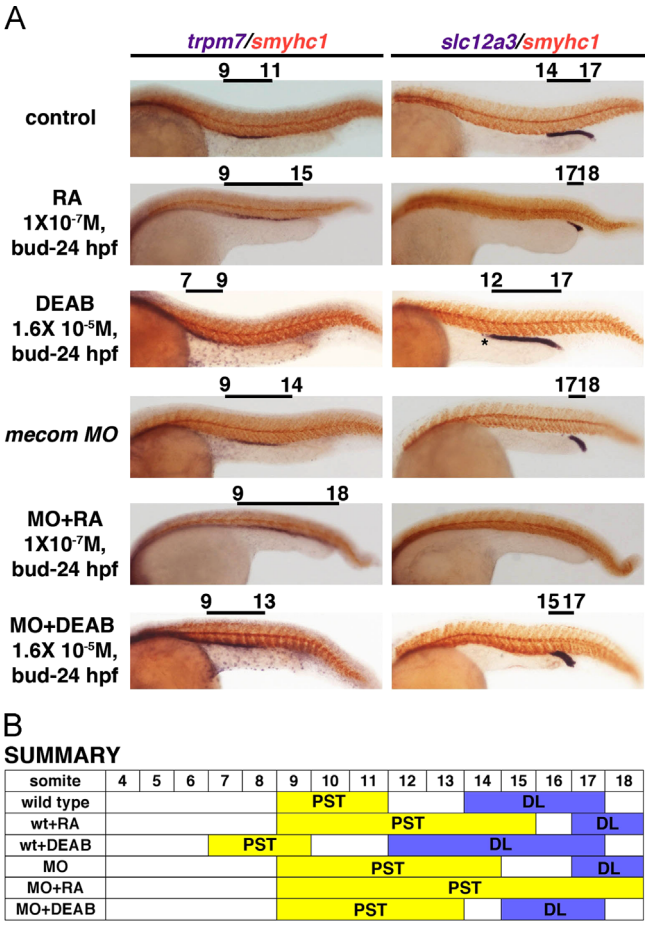

Fig. 5. *mecom* and RA have opposing roles in PST and DL formation during proximodistal segmentation of the pronephros. (A) Wild type embryos or *mecom* morphants were incubated with 1×10^{-7} M RA, 1.6×10^{-5} M DEAB or DMSO. WISH using the PST marker *trpm7* and DL marker *slc12a3* showed that exogenous RA resulted in a more severe segmental phenotype in the *mecom* morphant pronephros, with further expanded PST and reduced DL. DEAB treatment partially rescued the segmentation phenotype in *mecom* morphants. (B) Schematic summary of segmentation changes in wild type embryos, *mecom* morphants, and wild type embryos or morphants treated with RA or DEAB. Yellow and blue boxes highlight the PST and DL segments, respectively.

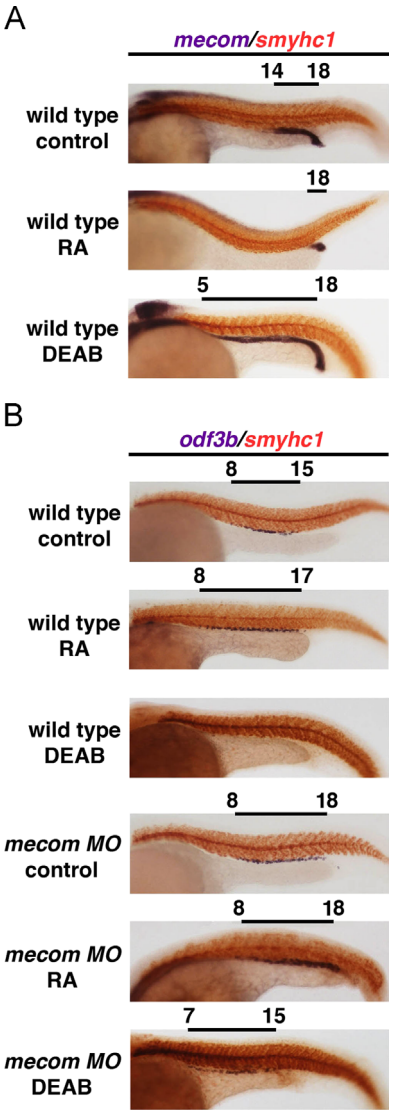

Fig. 6. RA negatively regulates *mecom*, which enables MCC formation. (A) Wild type embryos treated with 1×10^{-7} M RA, 1.6×10^{-5} M DEAB or DMSO. Analysis of *mecom* transcripts using WISH shows that RA treatment diminishes the *mecom* domain while abrogation of RA signaling expands the *mecom* domain. (B) MCCs were labeled by *odf3b* in wild types and *mecom* morphants treated with RA or DEAB. *mecom* knockdown resulted in a caudal shift of MCC domain in the DL and PD regions, and this effect was partially rescued by treating morphant embryos with DEAB. Notably, wild type embryos treated with DEAB had abolished MCC formation, while RA induced ectopic MCC formation in the distal region of the pronephros.

To determine if RA is required for MCC progenitor formation during early nephrogenesis, we exposed embryos to DEAB to inhibit RA synthesis. Wild type embryos treated with DEAB from 75% epiboly to 24 hpf, at the concentration documented to induce proximodistal segmentation changes in the pronephros (Wingert et al., 2007), displayed a complete loss of MCCs at 24 hpf (Figs. 6B and S7). Consistent with the notion that RA is required for MCC formation, *lightbulb (lib)* embryos that have a mutation in the RA biosynthesis gene *aldehyde dehydrogenase 1a2* (Wingert and Davidson, 2011) showed a reduction in the MCC domain (Fig. S9). Next, we further tested the relationship between *mecom* and RA in MCC formation. Since our findings thus far indicated that *mecom* represses MCCs, and RA represses *mecom*, we hypothesized that DEAB treatment had abrogated MCC formation due to the elevated *mecom* expression (Fig. 6A). In keeping with this, DEAB-treated *mecom* morphants developed MCCs (Figs. 6B and S7). These results indicate that alleviating the inhibitory effect of *mecom* on MCC differentiation is sufficient to reverse the MCC deficiency that results from an absence of RA signaling. Taken together, these data suggest that there is an exquisite interplay involving RA and *mecom* that titrates MCC formation: essentially, that RA acts to inhibit *mecom*, while *mecom* inhibits MCC fate choice.

mecom and Notch signaling coordinate MCC density in the zebrafish pronephros

In the pronephros tubules, MCCs are dispersed among the single-ciliated transporting epithelia in a 'salt-and-pepper' pattern (Ma and Jiang, 2007; Liu et al., 2006). Notch signaling creates this cell distribution by controlling the MCC fate decision through a mechanism of Notch-mediated lateral inhibition (Ma and Jiang, 2007; Liu et al., 2006). During pronephros differentiation, MCC progenitors expressing the Notch ligand *jag2a* exclusively repress MCC fate in neighboring cells, leading them to acquire a transporting epithelial fate (Ma and Jiang, 2007; Liu et al., 2006). The γ-secretase inhibitor DAPT has been shown to effectively block Notch signaling and causes increased MCC numbers to form during nephrogenesis (Ma and Jiang, 2007; Liu et al., 2006). Based on the discovery that RA levels affect MCC formation, we first

addressed the relationship between RA and Notch signaling in modulating MCC fate. Changes in RA levels during mid-gastrulation (between 60% and 70% epiboly) alter proximodistal segmentation (Wingert et al., 2007; Wingert and Davidson, 2011), while changes in Notch affect MCC differentiation at slightly later times (90% epiboly to bud stages) (Ma and Jiang, 2007; Liu et al., 2006). Thus, it is very likely that RA acts upstream of Notch in MCC formation. MCC formation was evaluated when embryos were treated with RA or a combination of RA and expression of the Notch1a intracellular domain (NICD) under heat-shock control using a transgenic line Tg(*hsp70:gal4; uas:notch1a-intra*) (Fig. S10). RA treatment shifted the MCC domain posteriorly in non-transgenic NICD siblings (Fig. S10). This was consistent with the change in proximodistal segment domains after RA treatment in wild types (Fig. 5), and confirmed our prior observation (Fig. 6B). Dual RA treatment and NICD heat-shock caused a similar MCC domain posterior shift, but the number of MCCs was reduced (Fig. S10). This confirms that Notch acts as a repressor of MCC fate, and is consistent with the notion that RA treatment causes a diminution of Notch signaling that increases MCC formation in the pronephros.

Next, we hypothesized that *mecom* might interact with Notch to mediate the MCC epithelial fate choices because *mecom* morphants showed an increase in MCC density similar to the effect of blocking Notch signaling (Ma and Jiang, 2007; Liu et al., 2006). To compare the effects of *mecom* and Notch on MCC differentiation, MCC number was evaluated in *mecom* morphants and DAPT treated wild types using the ciliogenesis marker *odf3b*. As noted previously, the MCC domain shift in *mecom* morphants correlated with the alteration in segment sizes, and there was a significant increase of MCC density compared to wild types at 24 hpf (Fig. 7). To assess MCC quantity, the number of MCCs was quantified per every 10 μm in single nephrons. MCC density in *mecom* morphants was increased by 50% compared to wild types (Fig. 7). As reported (Ma and Jiang, 2007; Liu et al., 2006), wild type embryos treated with DAPT exhibited an increased MCC density (Fig. 7). In addition, whereas MCCs are regularly dispersed in a salt-and-pepper array within the wild type nephron, large MCC aggregates were observed both in DAPT-treated wild types and *mecom* morphant nephrons (Fig. 7). *mecom* morphants incubated with DAPT did not show any further increase in MCC density compared to *mecom* morphants or embryos treated with DAPT treatment alone (Fig. 7).

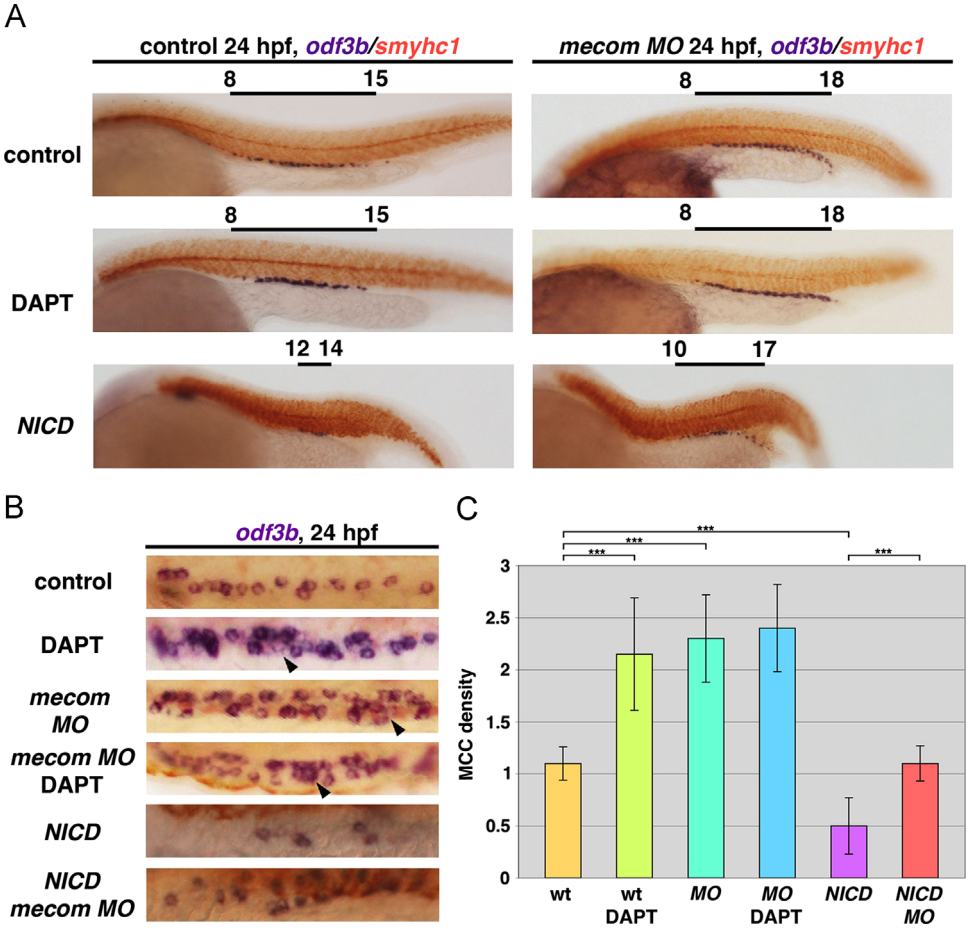

Fig. 7. *mecom* acts upstream of Notch signaling to modulate MCC differentiation and regulate the MCC domain. (A) Wild type embryos treated with 100 μM DAPT showed a significant increase of MCC number without ectopic MCC formation. *mecom* knockdown led to a caudal expansion of MCC in the DL and PD, and exhibited increased MCC density compared to wild types. A similar condensed MCC arrangement could also be seen in *mecom* morphants treated with DAPT. The overexpression of Notch1a resulted in decreased MCCs in heatshock induced *Tg*(*hsp70:gal4*; *uas:notch1a-intra*) embryos. Ectopic MCC formation associated with *mecom* knockdown was abolished by Notch signaling activation, though the domain of MCCs was still expanded. (B) Differentiated MCCs at 24 hpf under 10× magnification in a single nephron from wild types, wild types treated with DAPT, *mecom* morphants and morphants treated with DAPT, and finally wild types and *mecom* morphants with NICD overexpression. Note: MCCs displayed a condensed organization/cluster pattern in DAPT-treated wild type and *mecom* morphant pronephros, while DAPT treatment in *mecom* morphants failed to induce further MCC density. Arrows indicate large MCC aggregates observed in DAPT-treated wild types, *mecom* morphants, and DAPT-treated *mecom* morphants, which were absent from the wild type pronephros. For each experiment, at least 20 embryos were examined. (C) Quantification of MCC density in wild types, wild type embryos treated with DAPT, *mecom* morphants, and *mecom* morphants treated with DAPT. The Student *t*-test revealed significant increase of MCC density in DAPT treated wild types and *mecom* morphants relative to untreated wild types (***$p=0.0005$). Alterations of MCC density between *mecom* morphants and morphants treated with DAPT did not reach statistical significance. For each experiment, at least 20 embryos were examined.

Further, disrupting Notch signaling in *mecom* morphants with DAPT did not induce additional condensed MCC numbers (Fig. 7). Taken together, these results show that there is no additive effect of *mecom* and Notch signaling in modulating MCC differentiation. As such, we hypothesized that *mecom* and Notch signaling may collaborate in the same pathway to limit MCC formation, with additional roles of *mecom* to precisely define MCC territory in the pronephros.

To address whether *mecom* acts upstream or downstream of Notch signaling in modulating MCC differentiation, we utilized Notch transgenic lines to investigate whether MCC expansion could be ameliorated in *mecom* morphants with ectopic Notch signaling. We again used the double transgenic line Tg(*hsp70:gal4; uas:notch1a-intra*) to overexpress NICD with heat-shock induction. NICD activation by heat-shocking transgenic embryos at the bud stage resulted in fewer MCCs compared with control siblings (Fig. 7), consistent with published results (Liu et al., 2006). Strikingly, transgenic NICD activation in *mecom* morphants reduced MCC numbers, thus successfully rescuing the aggregate MCC phenotype (Fig. 7). These results provide evidence that Notch signaling acts downstream of *mecom* to restrict MCC formation during the choice between MCC and transporting epithelia fates. Overall, these studies show that *mecom* is a vital component of the gene regulatory network that controls MCC development.

Discussion

Herein we uncovered a fundamental role of *mecom* in modulating proximodistal segmentation and MCC fate choice during zebrafish nephrogenesis (Fig. 8A). Given the presence of *mecom* transcripts in a shifting caudal domain of the renal progenitors during the time period when nephron segmentation is established (through to 24 hpf), we speculate that *mecom* could act in multiple places and times to restrict the PST and promote the DL, respectively. The onset of *mecom* expression was detected at the 3-somite stage in the caudal domain of the renal progenitor field, in a non-overlapping pattern with the *dlc*-expressing rostral domain. This provides molecular evidence for renal progenitor specification several hours earlier in somitogenesis than previously documented (Gerlach and Wingert, 2013). However, this finding is consistent with the observation that modulations in RA levels during mid to late gastrulation have consequences for nephron proximodistal pattern (Gerlach and Wingert, 2013). The *mecom* expression domain later undergoes an incredibly progressive and dynamic shift toward the caudal end of the renal progenitor field before its restriction to the DL–PD at 24 hpf. Based on the presence of *mecom* transcripts in central and caudal renal progenitors, we hypothesize that *mecom* functions in proximodistal segmentation to promote DL induction and restrict the PST field during nephrogenesis (Fig. 8A).

In addition, we have determined several new roles and relationships between *mecom*, RA, and Notch signaling during MCC fate choice along the pronephros (Fig. 8B). We found that *mecom* morphants exhibit increased MCC numbers, demonstrating that *mecom* is needed to repress MCC fate choice. Blocking RA signaling by treating embryos with DEAB completely prevented MCC formation, and this inhibitory effect was alleviated by knocking down *mecom*. These data suggest that RA signaling promotes/enables MCC formation through *mecom* inhibition. Further, our studies place *mecom* upstream of Notch, since MCC expansion in *mecom* morphants was rescued by inducing Notch signaling. Based on these findings, we conclude that RA is crucial for MCC progenitor formation by limiting *mecom* activity, and that *mecom* in turn provides an inhibitory effect on MCC formation through promoting Notch signaling to regulate the balance of MCC-transporting epithelia fate choice (Fig. 8B). Also, since RA treatment can expand the MCC domain in *mecom* morphants, this suggests that there could be other factor(s) downstream of RA, possibly in parallel with *mecom*/Notch, that contribute to the positive role of RA in promoting MCC differentiation (Fig. 8B). Additional studies are needed to address how *mecom* coordinates both proximodistal segmentation and MCC fate choice – such as whether these are actually independent or overlapping pathways. Nevertheless, our data suggest that the proper dosage of RA, *mecom*, and Notch is absolutely essential for normal nephrogenesis.

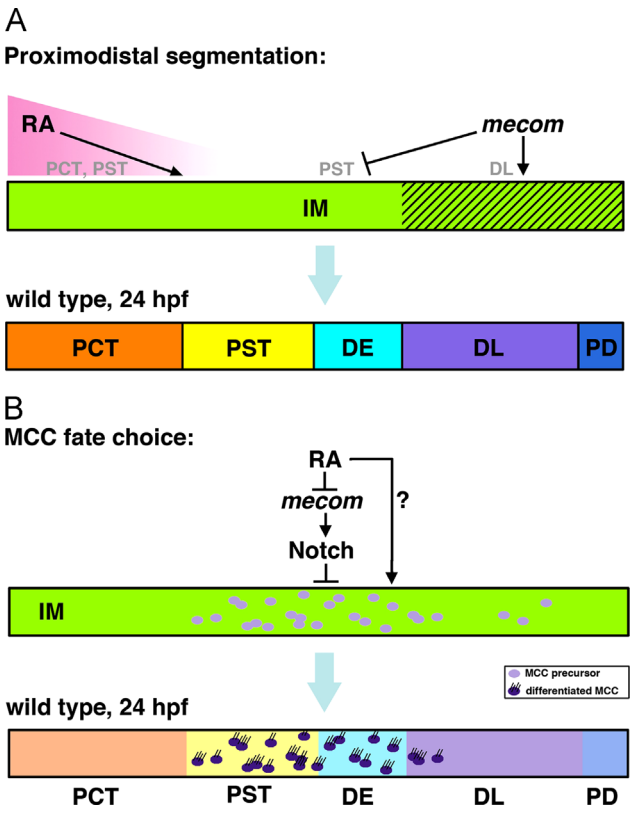

Fig. 8. Model of *mecom* function during nephrogenesis. (A) Role(s) of *mecom* during pronephros proximodistal segmentation. At early somitogenesis, forming somites generate a gradient of RA, which diffuses along the IM and modulates proximodistal patterning of the renal progenitors by promoting proximal segmentation and restricting distal fates. Initially expressed in the caudal domain of the renal progenitor field, *mecom* is negatively regulated by RA signaling and executes a contrary role to that of RA by favoring distal tubule formation and/or limiting proximal segmentation. Interplays between RA and *mecom*, as well as other transcription factors and signaling pathways precisely define the patterning of the renal progenitors during nephrogenesis, which develops into a pronephros with at least eight distinct segments by 24 hpf. *mecom* is specifically essential to promote the DL and possibly to restrict the PST. (B) RA, *mecom*, and Notch activities coordinate MCC formation. RA signaling is required for MCCs to develop, and one modality is that RA acts to negatively regulate *mecom* expression. RA likely has other targets that promote MCC formation, which remain unidentified. To further refine the balance between MCC and transporting epithelia fate choice, *mecom* represses ectopic MCC formation by promoting Notch signaling. Notch is the penultimate signal that inhibits MCC induction via lateral inhibition. By 24 hpf, MCCs are dispersed along the pronephric tubules in PST, DE, and DL regions adopting a proper 'salt-and-pepper' fashion. Abbreviations: RA (retinoic acid), PCT (proximal convoluted tubule), PST (proximal straight tubule), MCC (multiciliated cell), DE (distal early), DL (distal late), and PD (pronephric duct).

Mechanisms of mecom function during zebrafish nephrogenesis

The molecular mechanism of *mecom* in regulating pronephros segmentation and epithelial fate decision remains intriguing. In mammals, the *Mecom* gene is characterized as one of the splice variants of the gene *Evi1*, a conserved zinc finger transcription

factor crucial for both development and oncogenesis (Wieser, 2007). The *Mecom* transcript consists of extra sequence from the upstream *Mds1* gene, resulting in a 188 amino acid extension encoding a PR domain homologous to the SET protein methyltransferase domain (Wieser, 2007). The SET domain-containing proteins are a family of epigenetic regulators responsible for most histone lysine methylation (Dillon et al., 2005). A genome-wide survey of zebrafish SET domain-containing gene revealed *mecom* (referred to as *prdm3*) as a member of the SET domain-containing proteins (Sun et al., 2008). It is not known, however, whether the PR domain encoded by the zebrafish *mecom* sequence possesses histone methyltransferase activity.

The presence of zinc finger domains and their potentials to bind specific DNA sequences suggests *mecom* may function as a transcription factor to directly modify gene activities. However, target genes of *mecom* responsible for kidney development have yet to be identified. The presence of several consensus binding sites of co-activators and co-repressors in the Mecom protein argue additional biochemical role of *mecom* as a transcription co-factor (Wieser, 2007). Indeed, *mecom* has been shown to participate in chromatin modification by interacting with CtBP co-repressor or histone deacetylases (HDACs) (Wieser, 2007). In *Drosophila*, the *mecom* homologous gene *hamlet* controls olfactory receptor neuron diversification via locus-specific histone methylation at the Notch target promoter (Endo et al., 2012). In vertebrates, the highly related *mecom* variant *evi1* has been shown to repress BMP/Smad-mediated activation of endogenous genes required for cell fate specification. In this case, Evi1 and CtBP are recruited to target gene promoter upon TGFβ stimulation, leading to decreased histone acetylation and transcription (Alliston et al., 2005). Notably, chromatin modification seems to be crucial for proper nephron development, as inhibition of HDAC in zebrafish embryos results in the expansion of the renal progenitor cell population (de Groh et al., 2010).

Several studies suggest that mammalian *Mecom* affects cellular proliferation and differentiation in cell-type specific manners (Wieser, 2007). Therefore, in the developing pronephros, one possibility that we have not yet explored is that *mecom* fulfills its function by interfering with renal progenitor proliferation and/or differentiation. Further, the persistence of *mecom* transcripts in the DL and PD at 24 hpf could serve later roles in nephron morphogenesis – which might partly explain renal failure in *mecom* morphants. Recent studies have reported elevated epithelial proliferation in the distal tubule and duct at 3–4 days post-fertilization, which serves as a compensatory mechanism allowing for complex morphological change in the proximal segments driven by collective cell migration toward the glomerulus (Vasilyev et al., 2009, 2012). Thus, persistent *mecom* expression in the DL segment and PD at 24 hpf may account for active cell proliferation in these regions and in turn facilitate nephron morphogenesis post-segmentation events. Interestingly, the overexpression of *Mecom* in *Xenopus* repressed proximal fates and glomerulus formation, while inactivation of *Mecom* by fusing the wild type protein with the VP16 activation domain disrupted pronephros duct development (van Campenhout et al., 2006). In light of our findings, Mecom activity may be a conserved requirement in distal nephron development, though additional studies are needed to explore this possibility.

The elucidation of new roles that RA plays during zebrafish nephrogenesis

RA is a key modulator of pronephros development in the zebrafish (Gerlach and Wingert, 2013). RA signaling is required between gastrulation and early somitogenesis to induce podocytes and proximal segmental fates and to inhibit expansion of distal segments (Wingert, et al., 2007). RA generated in the anterior paraxial mesoderm (PM) is hypothesized to diffuse to the adjacent renal progenitors that give rise to the pronephros (Wingert et al., 2007; Wingert and Davidson, 2011). Since the rostral-most PM produces RA first, the current model is that a gradient of RA is generated along the IM, which provides higher levels of RA in the rostral region that induce proximal fates, while low RA levels in the caudal region allow distal segment formation (Wingert et al., 2007; Wingert and Davidson, 2008, 2011). Furthermore, growing evidence suggests transcription factors essential for nephron development act downstream of RA during pronephric segmentation patterning. For example, the homeodomain transcription factor *irx3b* has been shown to modulate DE formation and PCT/PST boundary establishment downstream of RA (Wingert and Davidson, 2011).

Several studies support the existence of a regulatory relationship between RA and *Mecom*. In mammalian cell culture studies, all-trans RA was shown to activate the *Mecom* locus via a consensus RARE located in exon 1a of the human *Evi1* gene (Bingemann et al., 2009). Meanwhile, RA also induced *mecom* expression indirectly through unknown mechanisms (Bingemann et al., 2009). In the *Xenopus* pronephros, exogenous RA is associated with elevated *Mecom* transcript levels (van Campenhout et al., 2006). In contrast, our analysis reveals that RA signaling inhibits *mecom* expression in the zebrafish pronephros. Since *mecom* is expressed in zebrafish pronephros renal progenitors starting from the onset of nephrogenesis, *mecom* could be a direct or indirect target of RA signaling. A better understanding of the relationship between RA and *mecom* will help to elucidate how these factors and/or their targets interact to precisely define the pronephros segment pattern.

The link between RA signaling and MCC development has not been previously reported. In the zebrafish pronephros, the majority of pronephric epithelial cells bear single apical cilium, while MCCs represent a subset of epithelial cells that display up to 16 apical motile cilia. It has been demonstrated that Notch signaling regulates differentiation of transporting epithelia and MCCs in the zebrafish pronephros via lateral inhibition, where 'multiciliated progenitor cells' suppress transporting epithelia to acquire MCC fates possibly by expressing high levels of *jag2*, which interacts locally with Notch3 receptors present on transporting epithelial surface (Ma and Jiang, 2007; Liu, et al., 2006). Our data reveals that MCC fate choice is titrated through a concert of RA, *mecom*, and finally Notch signaling. Further experiments are needed to ascertain how *mecom* promotes Notch activity in renal progenitors. However, our work here adds several levels of complexity to the knowledge about how the MCC-transporting epithelia balance is regulated.

In conclusion, our studies have revealed new insights into the processes of nephron segmentation and cell fate choice during nephrogenesis. Given the similarities that exist between nephron segmental structure and ontogeny between zebrafish and other vertebrates, future analysis of *Mecom* function during mammalian renal development may provide novel information about nephron patterning in humans that could be relevant to understanding renal stem cell biology, kidney birth defects and other kidney diseases.

Author contributions

Conceived, designed, and performed experiments, and analyzed data: YL, CNC, VAV, and RAW. Wrote the manuscript: YL and RAW. Edited, revised and approved the final manuscript: YL, CNC, VAV, and RAW.

Acknowledgments

This work was supported by the following grants to RAW: NIH Grant K01DK083512, NIH Grant DP2OD008470, March of Dimes

Basil O'Connor Starter Scholar grant award #5-FY12-75, NIH Grant R01DK100237, and start up funding from the University of Notre Dame and College of Science. We are especially grateful to Elizabeth and Michael Gallagher for a generous gift to the University of Notre Dame on behalf of their family for the support of stem cell research. The funders had no role in the study design, data collection and analysis, decision to publish, or manuscript preparation. We thank Alan J. Davidson for his mentorship and support during the initiation of this project, and the Zon laboratory for the gift of Notch transgenic lines. We thank the staffs of the Department of Biological Sciences and the Center for Zebrafish Research at Notre Dame for their dedication and care of our zebrafish aquarium. Finally, we thank the members of our wonderful lab for their discussions and insights about this work.

Appendix. Supplementary materials

Supplementary data associated with this article can be found in the online version at http://dx.doi.org/10.1016/j.ydbio.2013.11.021.

References

Alliston, T., Ko, T.C., Cao, Y., Liang, Y.Y., Feng, X.H., Chang, C., Derynck, R., 2005. Repression of bone morphogenetic protein and activin-inducible transcription by Evi-1. J. Biol. Chem. 24, 24227–24237.

Bingemann, S.C., Konrad, T.A., Wieser, R., 2009. Zinc finger transcription factor ecotropic viral integration site 1 is induced by all-trans retinoic acid (ATRA) and acts as a dual modulator of the ATRA response. FEBS J. 276, 6810–6822.

Costantini, F., Kopan, R., 2010. Patterning a complex organ: branching morphogenesis and nephron segmentation in kidney development. Dev. Cell 18, 698–712.

de Groh, E.D., Swanhart, L.M., Cosentino, C.C., Jackson, R.L., Dai, W., Kitchens, C.A., Day, B.W., Smithgall, T.E., Hukriede, N.A., 2010. Inhibition of histone deacetylase expands the renal progenitor cell population. J. Am. Soc. Nephrol. 21, 794–802.

Dillon, S.C., Zhang, X., Trievel, R.C., Cheng, X., 2005. The SET-domain protein superfamily: protein lysine methyltransferases. Genome Biol. 6, 227.

Dressler, G.R., 2006. The cellular basis of kidney development. Annu. Rev. Cell Dev. Biol. 22, 509–529.

Duester, G., 2008. Retinoic acid synthesis and signaling during early organogenesis. Cell 134, 921–931.

Drummond, I.A., Majumdar, A., Hentschel, H., Elger, M., Solnica-Krezel, L., Schier, A. F., Neuhauss, S.C., Stemple, D.L., Zwartkruis, F., Rangini, Z., Driever, W., Fishman, M.C., 1998. Early development of the zebrafish pronephros and analysis of mutations affecting pronephric function. Development 125, 4655–4667.

Endo, K., Karim, M.R., Taniguchi, H., Krejci, A., Kinameri, E., Siebert, M., Ito, K., Bray, S.J., Moore, A.W., 2012. Chromatin modification of Notch targets in olfactory receptor neuron diversification. Nat. Neurosci. 15, 224–233.

Gerlach, G.F., Wingert, R.A., 2013. Kidney organogenesis in the zebrafish: insights into vertebrate nephrogenesis and regeneration. WIREs Dev. Biol. 2, 559–585.

Goyama, S., Yamamoto, G., Shimabe, M., Sato, T., Ichikawa, M., Ogawa, S., Chiba, S., Kurokawa, M., 2008. Evi-1 is a critical regulator for hematopoietic stem cells and transformed leukemic cells. Cell Stem Cell 3, 207–220.

Hoyt, P.R., Bartholomew, C., Davis, A.J., Yutzey, K., Gamer, L.W., Potter, S.S., Ihle, J.N., Mucenski, M.L., 1997. The Evi1 proto-oncogene is required at midgestation for neural, heart, and paraxial mesenchyme development. Mech. Dev. 65, 55–70.

Kimmel, C.B., Ballard, W.W., Kimmel, S.R., Ullmann, B., Schilling, T.F., 1995. Stages of embryonic development of the zebrafish. Dev. Dyn. 203, 253–310.

Little, M.H., Mc Mohan, A.P., 2012. Mammalian kidney development: principles, progress, and projections. Cold Spring Harb. Perspect. Biol. 4 (5), http://dx.doi.org/pii:008300.

Liu, Y., Pathak, N., Kramer-Zucker, A., Drummond, I.A., 2006. Notch signaling controls the differentiation of transporting epithelia and multiciliated cells in the zebrafish pronephros. Development 134, 1111–1122.

Ma, M., Jiang, Y.J., 2007. Jagged2a-Notch signaling mediates cell fate choice in the zebrafish pronephric duct. PLoS Genet. 3 (1), e18.

Mead, P.E., Parganas, E., Ohtsuka, S., Morishita, K., Gamer, L., Kuliyev, E., Wright, C. V., Ihle, J.N., 2005. Evi-1 expression in Xenopus. Gene Expr. Patterns 5, 601–608.

Naylor, R.W., Przepiorski, A., Ren, Q., Yu, J., Davidson, A.J., 2013. HNF1B is essential for nephron segmentation during nephrogenesis. J. Am. Soc. Nephrol. 24, 77–87.

Pfeffer, P.L., Gerster, T., Lun, K., Brand, M., Busslinger, M., 1998. Characterization of three novel members of the zebrafish *Pax2/5/8* family and dependency of *Pax5* and *Pax8* expression on the *Pax2.1* (*noi*) function. Development 125, 3063–3074.

Scheer, N., Campos-Ortega, J.A., 1999. Use of the Ga14-UAS technique for targeted gene expression in the zebrafish. Mech. Dev. 80, 153–158.

Serluca, F.C., Fishman, M.C., 2001. Pre-pattern in the pronephric kidney field of zebrafish. Development 128, 2233–2241.

Sun, X.J., Xu, P.F., Zhou, T., Hu, M., Fu, C.T., Zhang, Y., Jin, Y., Chen, Y., Chen, S.J., Huang, Q.H., Liu, T.X., Chen, Z., 2008. Genome-wide survey and developmental expression mapping of zebrafish SET domain-containing genes. PLoS One 3, e1499.

van Campenhout, C., Nichane, M., Antoniou, A., Pendeville, H., Bronchain, O.J., Marine, J.C., Mazabraud, A., Voz, M.L., Bellefroid, E.J., 2006. Evi1 is specifically expressed in the distal tubule and duct of the Xenopus pronephros and plays a role in its formation. Dev. Biol. 294, 203–219.

Vasilyev, A., Liu, Y., Mudumana, S., Mangos, S., Lam, P.Y., Majumdar, A., Zhao, J., Poon, K.L., Kondrychyn, I., Korzh, V., Drummond, I.A., 2009. Collective cell migration drives morphogenesis of the kidney nephron. PLoS Biol. 7 (1), e9.

Vasilyev, A., Liu, Y., Hellman, N., Pathak, N., Drummond, I.A., 2012. Mechanical stretch and PI3K signaling link cell migration and proliferation to coordinate epithelial tubule morphogenesis in the zebrafish pronephros. PLoS One 7 (7), e39992.

Wieser, R., 2007. The oncogene and developmental regulator EVI1: expression, biochemical properties, and biological functions. Gene 15, 346–357.

Wingert, R.A., Brownlie, A., Galloway, J.L., Dooley, K., Fraenkel, P., Axe, J., Barut, B., Davidson, A.J., Noriega, L., Sheng, X., Zhou, Y., Zon, L.I., 2004. The *chianti* zebrafish mutant provides a model for erythroid-specific disruption of transferrin receptor 1. Development 131, 6225–6235.

Wingert, R.A., Davidson, A.J., 2008. The zebrafish pronephros: a model to study segmentation. Kid. Int. 73, 1120–1127.

Wingert, R.A., Selleck, R., Yu, J., Song, H.D., Chen, Z., Song, A., Zhou, Y., Thisse, B., Thisse, C., McMahon, A.P., Davidson, A.J., 2007. The *cdx* genes and retinoic acid control the positioning and segmentation of the zebrafish pronephros. PLoS Genet. 3, 1922–1938.

Wingert, R.A., Davidson, A.J., 2011. Zebrafish nephrogenesis involves dynamic spatiotemporal expression changes in renal progenitors and essential signals from retinoic acid and *irx3b*. Dev. Dyn. 240, 2011–2027.

Yu, J., Valerius, M.T., Duah, M., Staser, K., Hansard, J.K., Guo, J.J., McMahon, J., Vaughan, J., Faria, D., Georgas, K., Rumballe, B., Ren, Q., Krautzberger, A.M., Junker, J.P., Thiagarajan, R.D., Machanick, P., Gray, P.A., van Oudenaarden, A., Rowitch, D.H., Stiles, C.D., Ma, Q., Grimmond, S.M., Bailey, T.L., Little, M.H., McMahon, A.P., 2012. Identification of molecular compartments and genetic circuitry in the developing mammalian kidney. Development, 139; , pp. 1863–1873.

Zhang, Y., Stehling-Sun, S., Lezon-Geyda, K., Juneja, S.C., Coillard, L., Chatterjee, G., Wuertzer, C.A., Camargo, F., Perkins, A.S., 2011. PR-domain-containing Mds1–Evi1 is critical for long-term hematopoietic stem cell function. Blood 118, 3853–3861.